Acoustic Logging While Drilling(LWD): Experimental Studies with Anisotropic Models

V. N. Rama Rao, Zhenya Zhu, Daniel R. Burns, and M. Nafi Toksöz
Earth Resources Laboratory
Department of Earth, Atmospheric, and Planetary Sciences
Massachusetts Institute of Technology
Cambridge, MA 02139

Abstract

A model LWD tool (0.16" ID, 0.4" OD) was built to investigate its operation in an anisotropic formation. The tool consists of a dipole source and six dipole receivers capable of operating at several hundred kHz. The formation was a block of delabole slate with a borehole of 1.27 *cm* diameter.

In an anisotropic fluid-filled borehole with a dipole source and dipole receiver oriented along the principal directions, dipole (flexural) modes are mainly observed. Weak compression and shear refracted arrivals are also discernable when they were not obscured by stronger arrivals. Further, modes corresponding to fast shear direction are evident in the slow shear direction measurement.

With a model LWD tool in the fluid-filled borehole, and oriented in the fast and slow directions, the main arrivals were the corresponding flexural modes. Modes corresponding to the fast shear direction are no longer evident in the slow shear direction measurments. These preliminary experiments suggest that, with an LWD tool in an anisotropic formation, arrivals sensitive to formation properties can be discerned.

1 Introduction

With increasing pressures on improving exploration efficiency, LWD measurements are gaining in prominence, particularly in critical and expensive holes. Knowing the formation anisotropy and stress state impacts a variety of exploration and production decisions from casing design to preventing sanding, sustaining borehole stability, and planning stimulation treatments. The advantages of making formation measurements while drilling is that true stress estimates can be obtained prior to plastic deformation around the borehole, which can obscure the true stress state. Hence it is critical to understand the operation of LWD tool in anisotropic formations, be it instricsic or induced by the regional stress state.

The traditional wireline monopole well logging tool can excite and measure formation compressional and shear velocities in a hard formation (Tsang and Rader (1979); Cheng and

Toksöz (1981); Willis and Toksöz (1983)), but cannot excite shear wave directly in a soft formation (Winbow (1991)). A wireline dipole tool can generate a flexural wave in both hard or soft formation (Kurkjian and Chang (1986); Chen (1988)). At sufficiently low frequencies the velocity of the flexural wave is close to the formation shear velocity (Winbow (1991)). Further, the dipole source can excite a flexural wave in a cased borehole, whose velocity depends on that of the surrounding formation. In azimuthally anisotropic boreholes wireline cross-dipole tools have been used to measure formation anisotropy (Zhu et al. (1993); Alford (1986); Esmersoy et al. (1994); Sinha et al. (1994)).

An LWD tool in a borehole excites and measures arrivals related to formation properties and those that are due to the presence of the tool. Interpreting these measurements requires a knowledge of the potential modes that can be received and their propagation characteristics (Rao and Vandiver (1999); Rao et al. (1999)). To investigate the operation of the LWD tool in an anisotropic formation, a miniature tool and a model anisotropic formation (slate block) were built. The model tool had one dipole source and six dipole receivers. Transducer operation was first characterized through measurements in a water tank. Then a single source and receiver were positioned in the borehole, along the fast and slow shear directions, and measurements were made for different source-receiver separations. This was used to characterize the fluid-filled slate borehole. Then measurements were made with the tool in the borehole, to understand the effects of the tool and its operation in an anisotropic formation.

2 Model LWD Tool in an Anisotropic Borehole

A miniature LWD tool (0.16" ID, 0.4" OD) was constructed to investigate its operation in a variety of model formations. A dipole source and 6 dipole receivers are positioned as shown in Figure 1.

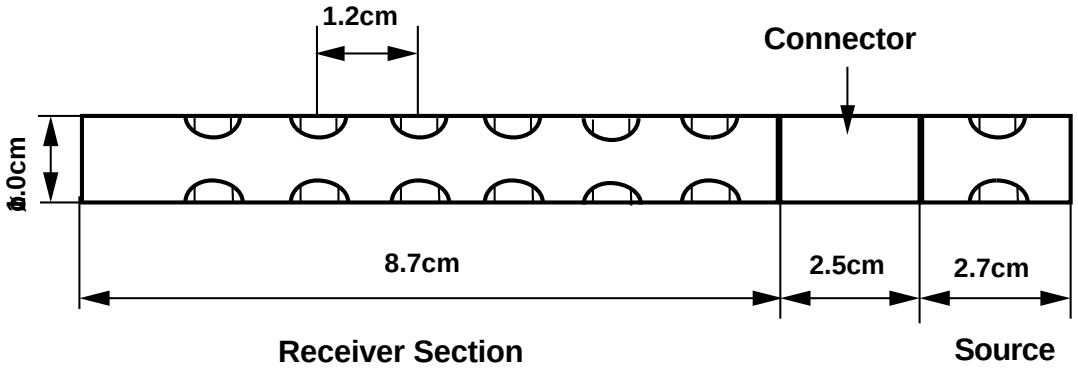

Figure 1: Schematic diagram of a dipole tool made of steel and the transducers shown in Figure 2.

2.1 Dipole transducers

In order to generate and receive flexural waves in a borehole model, we designed a dipole transducer, which operates in the ultrasonic frequency range.

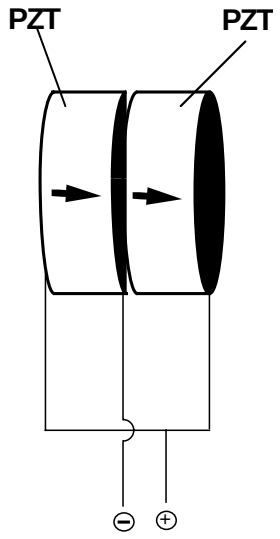

Figure 2: Schematic diagram of a dipole transducer. Two PZT crystal disks, with sides of like polarization glued together. Vibrating in piston mode the composite transducer behaves like a dipole. The "+" and "-" signs refer to the electrodes and the arrows refers to the direction of crystal polarization.

Figure 2 shows the structure of the dipole transducer created from two PZT disks. Each disk is a cylinder (0.635 cm in diameter and 0.37 cm in length) with a center frequency at free piston vibration of about 500 kHz. When the two disks are glued together with conducting epoxy, the center frequency of the composite transducer decreases to the 200-300 kHz range. The polarization of the two disks are in the same direction, so that the composite transducer operates in dipole mode. At a low power level, the transducer can be operated either as a source or as a receiver.

2.2 Tool characteristics

The transducer operation in the tool was characterized by recording the operation of the source and the receiver section separately. The source radiation and receiver response were measured in a water tank.

2.2.1 Source in a water tank

The expected radiation of the composite transducer should be akin to a dipole based on the structure and the vibration mode of the component crystal disks. A single sine wave pulse was used to excite the dipole source, and a hydrophone capable of receiving broadband signals was used to record the waveforms from both sides of the source. The radiation pattern

of the source confirms that the source transducer operates as a dipole. Further, mapping the amplitude of the hydrophone response as a function of frequency showed that the working frequency range of the source is 200-350 kHz.

2.2.2 Receivers in a water tank

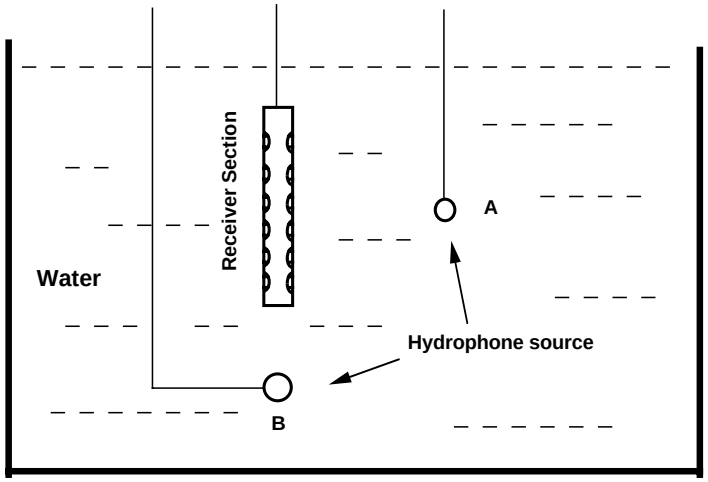

Figure 3: Schematic diagram for measurements in a water tank to check the consistency of the transducers on the receiver section. The source is a hydrophone which is located at position A and B. The six receivers record the waveforms.

The consistency of the six receiver transducers, were evaluated by measurements in a water tank, as shown in Figure 3. A hydrophone which is capable of broadband excitation operates as a source and is located at one side of the receiver section (position A) or under it (position B). The waveforms received by the six receivers are shown in Figure 4.

The amplitudes and shapes of the early cycles in Figure 4a are almost identical, because the distance between the source and each receiver is almost the same. Thus the response of the six receivers are consistent to excitation in a direction perpendicular to the axis of the tool. A second feature is that the receiver transducers ring for multiple cycles in response to a single cycle sine wave excitation, indicating low damping in the transducer construction. Since the same transducers are used as both sources and receivers, recorded waveforms will be narrowband, as is evident in the data.

When the hydrophone source is under the receiver section (position B in Figure 3), the receiver response decays with distance from source, as expected. Additionally it indicates that receptivity/radiation pattern of the dipole transducer, housed in the receiver section, is non-trivial in a direction perpendicular to its polarization.

2.3 Anisotropic borehole model

An anisotropic rock, Delabole slate, was used to construct a borehole model to investigate the operation of the model tool. The velocity distribution of the slate block is as shown in

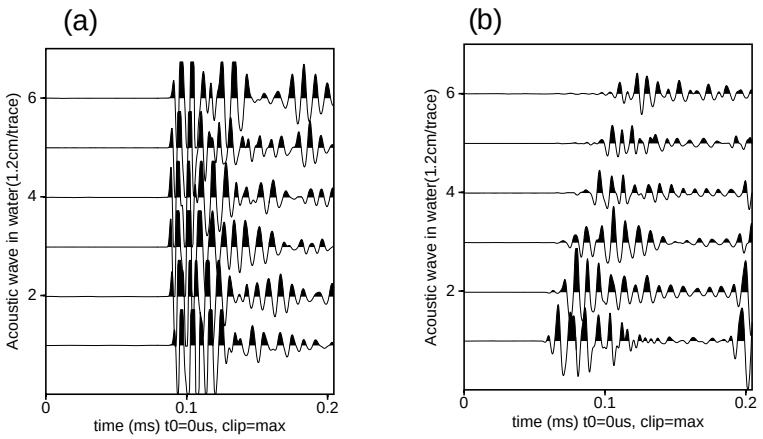

Figure 4: Acoustic waveforms recorded by the six dipole receivers when the hydrophone is at position A (a) and B (b) in Figure 3, respectively.

Figure 5. The density of slate is 2.65 g/cm^3 and its porosity is about 1%. It is strongly anisotropic with the relative anisotropy of 55.6% ((Vf-Vs)/Vs).

A borehole (1.27 cm dia) was drilled along its bedding creating an azimuthally anisotropic borehole. A shear wave propagating along the borehole has a phase speed of 4150 m/s if the particle motion is in the X-direction (fast direction) and a phase speed of 2650 m/s if it is in Y-direction (slow direction). An excitation at an arbitrary azimuthal orientation will excite two shear waves, one propagating as a fast shear wave and another as a slow shear wave.

3 Measurements in an Anisotropic Borehole

Two combinations of the tool are used to record waveforms generated by the dipole source. First, we use two unconnected dipole transducers, one as a source and one as a receiver and record the waveforms as the source receiver separation is changed. This would simulate measurements in a borehole without a tool. Then the model tool with a source and six receivers was used to make analogous measurements. In both cases, measurements were made with the source and receiver polarizations oriented along the fast and slow shear directions.

With dipole source and receivers in a borehole, arrivals corresponding to dipole modes can be expected. Theoretically, refracted compression and shear arrivals are not expected, as point dipole receivers would be insensitive to these axisymmetric arrivals. However, given the finite size of the transducers, the potential asymmetries in positioning them in the housing and the housing in the borehole, weak refracted arrivals are not uncommon in dipole receivers. Further, semblance processing, being mainly sensitive to coherence across the array and not to actual amplitudes of arrivals, can pick these refracted arrivals as long as they are not completely obscured by stronger arrivals.

To interpret the peaks in semblance, theoretical dispersion curves computed from a tool-in-a-borehole model are also presented. The formation modeled was isotropic, with shear

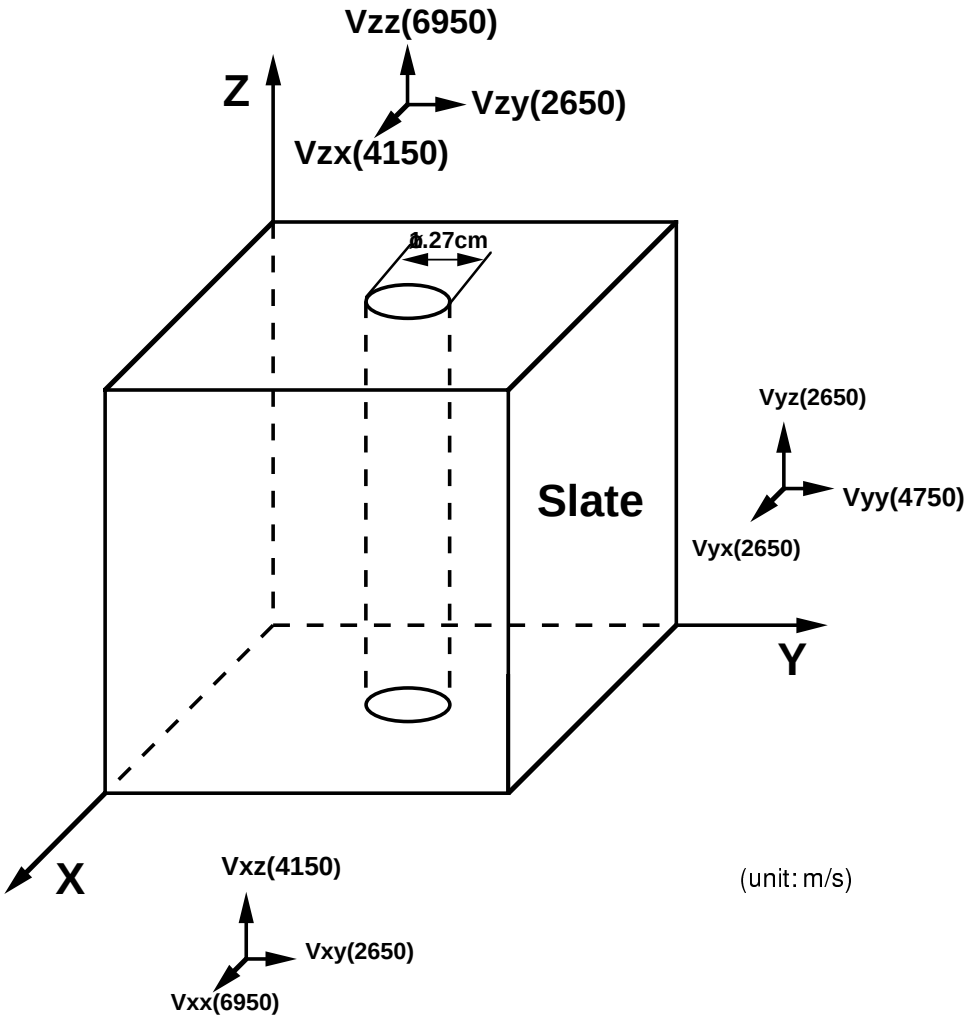

Figure 5: Schematic diagram of the Delabole slate model with a Z-direction borehole and 1.27 cm in diameter. Its compressional and shear velocities (m/s) along three directions are shown. The X direction is that of the fast shear wave and the Y-direction is that of slow shear wave.

speed equal to the fast (or slow) shear speed of slate and compression speed equal to that of slate. In the semblance plots, the curve (in white) corresponding to the locus where the phase speed is equal to the group speed is overlaid, to aid in identifying and interpreting of the arrivals. For example, the direct refracted arrivals will be located vertically at the corresponding formation speed, and horizontally, on or next to the line where phase speed equals group speed. The source center frequency was 250 kHz, with significant energy between 200-300 kHz. The intersection of this band with the various dispersion curves identifies the expected phase speed/group delay coordinates of the modes in the semblance plot.

3.1 Fluid-filled borehole

The dipole source and a single dipole receiver were positioned in a water-filled slate borehole, oriented along the fast and slow shear directions and data was recorded for different source receiver separations.

3.1.1 Fast shear direction

When the source and receiver are aligned in the fast shear direction, the observed waveforms and the corresponding semblance analysis is shown in Figure 6 while the relevant dispersion curves are in Figure 7.

The strong early arrivals correspond to the semblance peak labeled 1. This is the borehole flexural mode arrival, with the phase speed/group delay corresponding to this peak identified in Figure 7 as 1. As discussed earlier, the transducer response is narrowband, leading to a ringing response when excited by a single sine wave input. This results in the time spreading of the most arrivals, including the dominant arrival. Further, semblance analysis of such ringing waveforms gives rise to spurious peaks at discrete speeds, slower than the true speed (Briggs et al. (2002)) and are indicated as such in the semblance plots.

Another semblance peak identified as 2, corresponds to the fluid flexural mode arrival, labeled as 2 in Figure 7.

Of the three possible modes that can be excited around 250 kHz (Figure 7), two can be observed and this is a reflection of their corresponding excitation functions.

3.1.2 Slow shear direction

When the source and receiver are aligned in the slow shear direction, the observed waveforms and the corresponding semblance analysis is shown in Figure 8 while the relevant dispersion curves are in Figure 9.

The dominant arrivals that propagate along the receiver array correspond to the semblance peak 1. It is identified in the dispersion curves also as 1, and corresponds to the fluid flexural mode.

The two additional semblance peaks identified as 2 and 3 in Figure 8 are modal arrivals corresponding to the *fast shear* direction. The elongated peak 2, reflects the strong dispersive behavior of the inner fluid flexural mode (fast shear) in the neighborhood of the label 2 in Figure 7. At the arrival times corresponding to peak 2, the frequency content of the

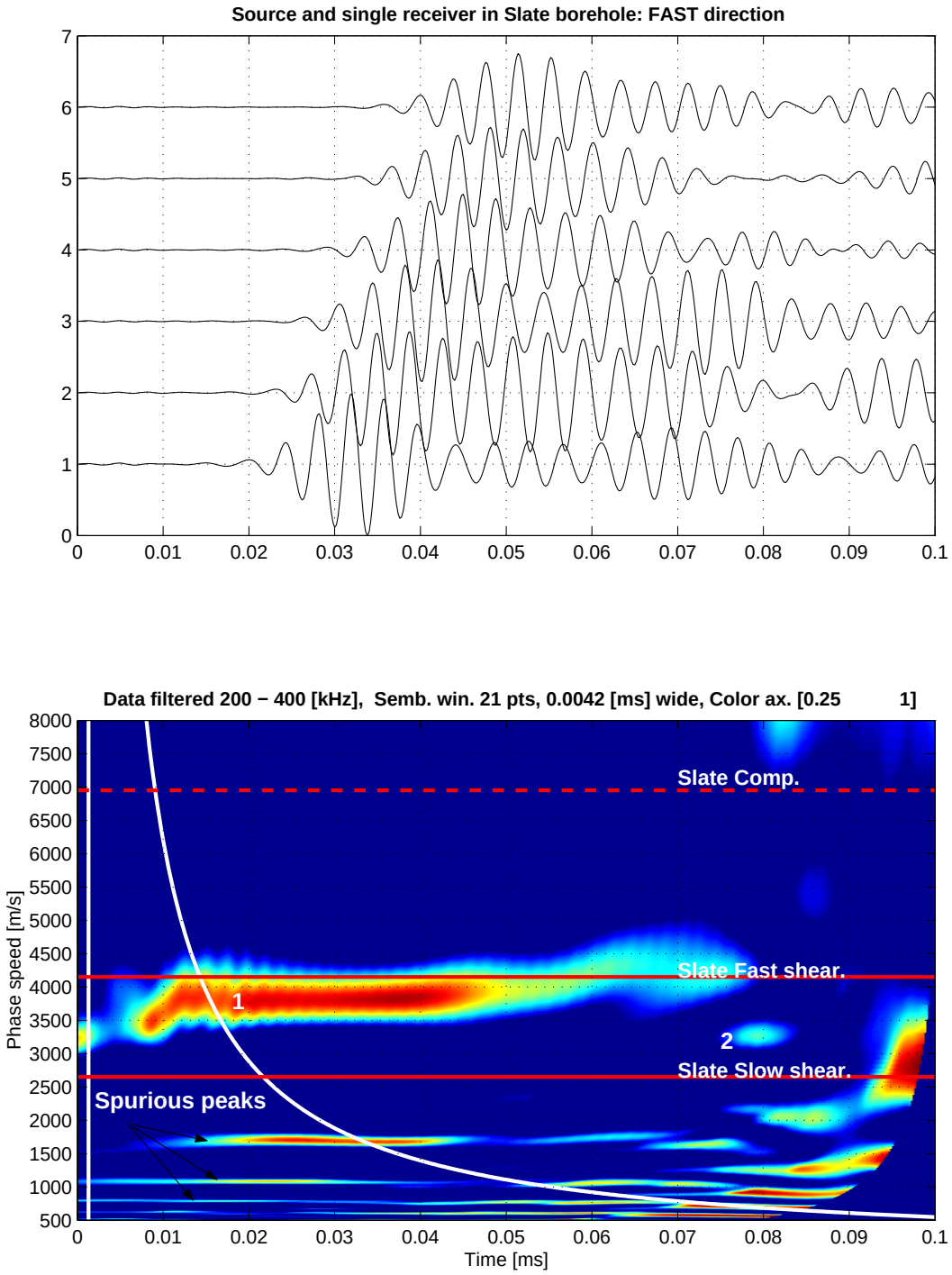

Figure 6: Source and receiver aligned in the fast shear direction in a slate borehole: Measured waveforms and semblance. The locus where phase speed is equal to group speed is identified by the white curve.

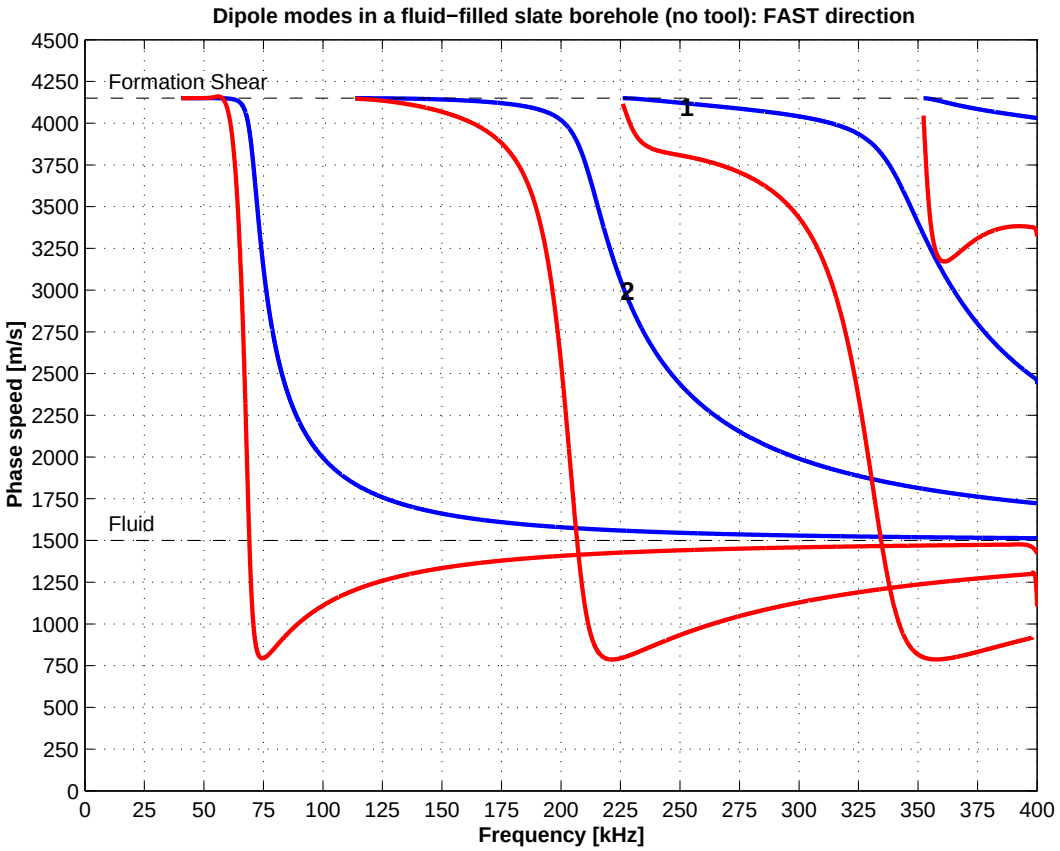

Figure 7: Dipole modes in an isotropic formation without tool. Formation shear speed is equal to the fast shear speed of slate and compression speed is equal to that of slate. Labels in the plot identify the dispersion character of correspondingly labeled arrivals/peaks in the semblance plot. (Phase speed—blue, group speed—red.)

waveforms decreases as time increases, corresponding to moving along that dispersion curve from about 250 - 225 kHz. Peak 3 is the the borehole flexural arrival (fast direction), but after reflection from the borehole boundary.

Additionally a clear semblance peak corresponding to a coherent but weak compressional refracted arrival is evident. Its arrival times that indicate that it is not a direct arrival, but has propagated from the source to the borehole boundary and reflected back. Direct refracted arrivals (compression or shear) are not observed because they are obscured by the the source ringing that is recorded in all receivers up to about 0.02 ms.

Of the three possible modes (slow shear) that can be excited around 250 kHz (Figure 9), one can be observed. Additionally two flexural modes belonging to the fast shear direction can be observed. The ratio of transducer diameter to the borehole diameter is large for the model compared to typical field situations. This makes the model transducers more likely to excite, and receive, modes corresponding to fast shear, in the slow shear direction. Overall, in the fast and slow shear direction measurements, the main arrivals can be interpreted as borehole flexural modal arrivals.

3.2 Tool in borehole

The complete tool, with a dipole source and six dipole receivers was placed in the slate borehole and data was recorded with the transducer polarizations oriented along the fast and slow shear directions.

3.2.1 Fast shear direction

When the source and receivers are aligned in the fast shear direction, the observed waveforms and the corresponding semblance analysis is shown in Figure 10 while the relevant dispersion curves are in Figure 11.

There is a dominant arrival with a phase speed near 4000 m/s, and between 0.015-0.03 ms (peak 1 in Figure 10), and this corresponds to the mode labeled 1 in Figure 11. Another peak at the same phase speed, but arriving later (0.06 ms) corresponds to this mode propagating away from the source, reflecting from the borehole boundary and propagating back to the receiver array. The peak at 1700 m/s and 0.025 ms is a spurious peak associated with the above ringing arrival.

The peaks, 2 and 3 in Figure 10, correspond to the modes labeled 2 and 3 in Figure 11. While the two labels appear on two unconnected dispersion curves, they correspond to the flexural behavior of the fluid column inside the tool (Rao et al. (1999)).

Finally, there is an weak but obvious compression refracted arrival at 0.065 ms. This corresponds to a compressional wave that has reflected from the boundary of the slate block. Compression refracted arrivals at early times are obscured by the ringing source signal. The remaining peaks do not correspond to modal or refracted arrivals and are likely modal arrivals reflected from the slate block boundaries.

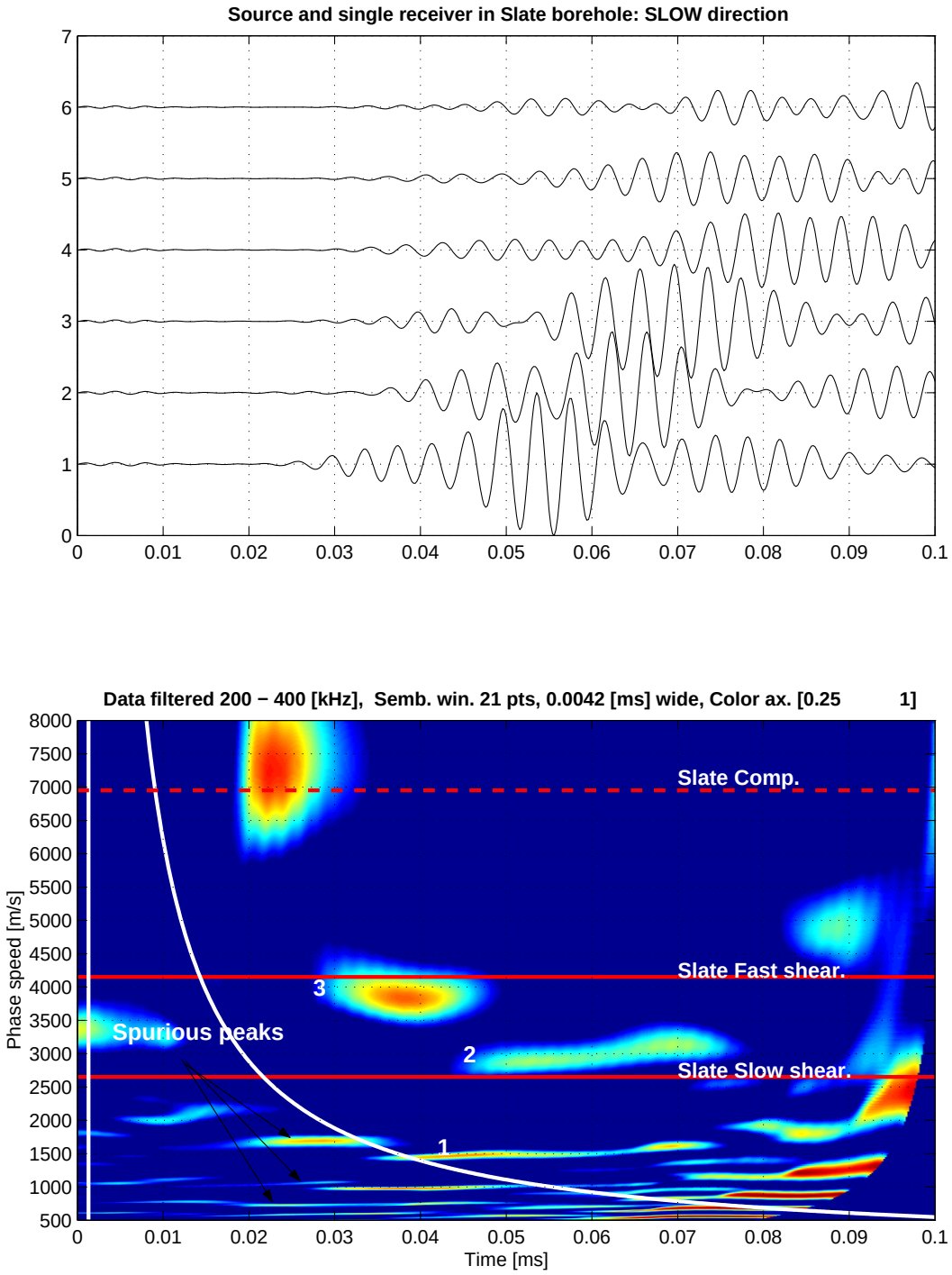

Figure 8: Source and a receiver aligned in the slow shear direction in a slate borehole: Measured waveforms and semblance. The locus where phase speed is equal to group speed is identified by the white curve.

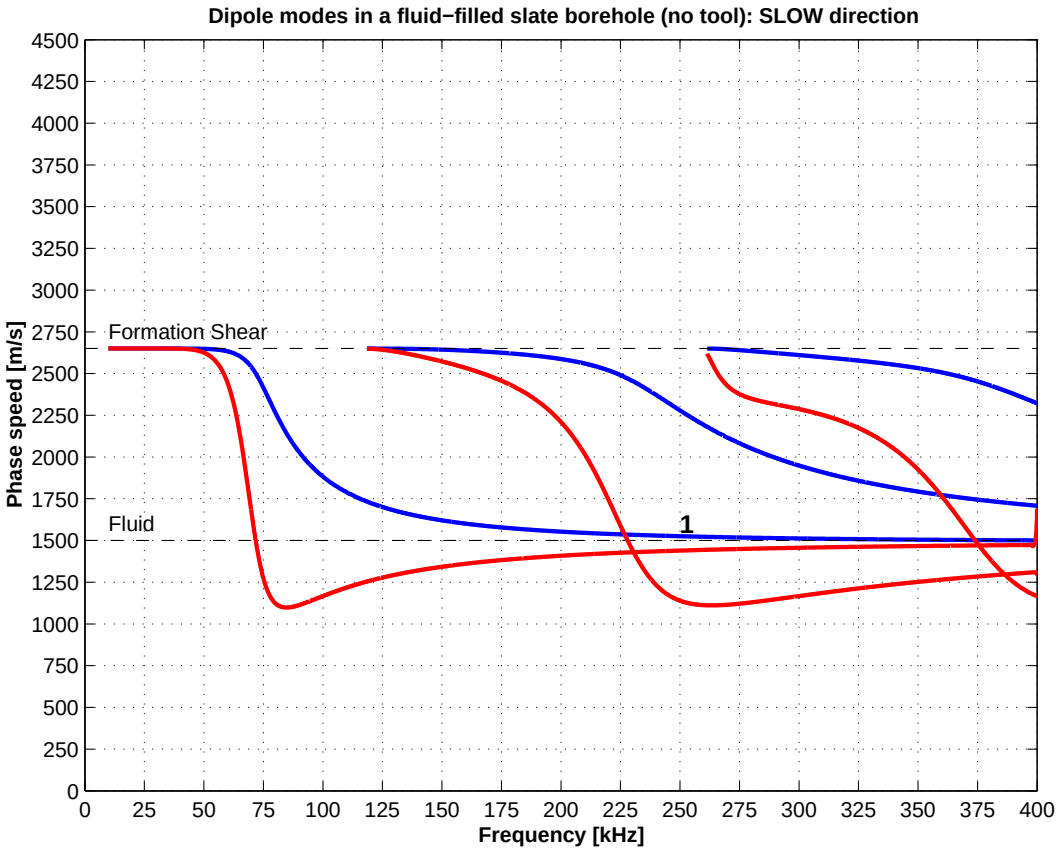

Figure 9: Dipole modes in an isotropic formation without a tool. Formation shear speed is equal to the slow shear speed of slate and compression speed is equal to that of slate. Labels in the plot identify the dispersion character of correspondingly labeled arrivals/peaks in the semblance plot. (Phase speed—blue, group speed—red.)

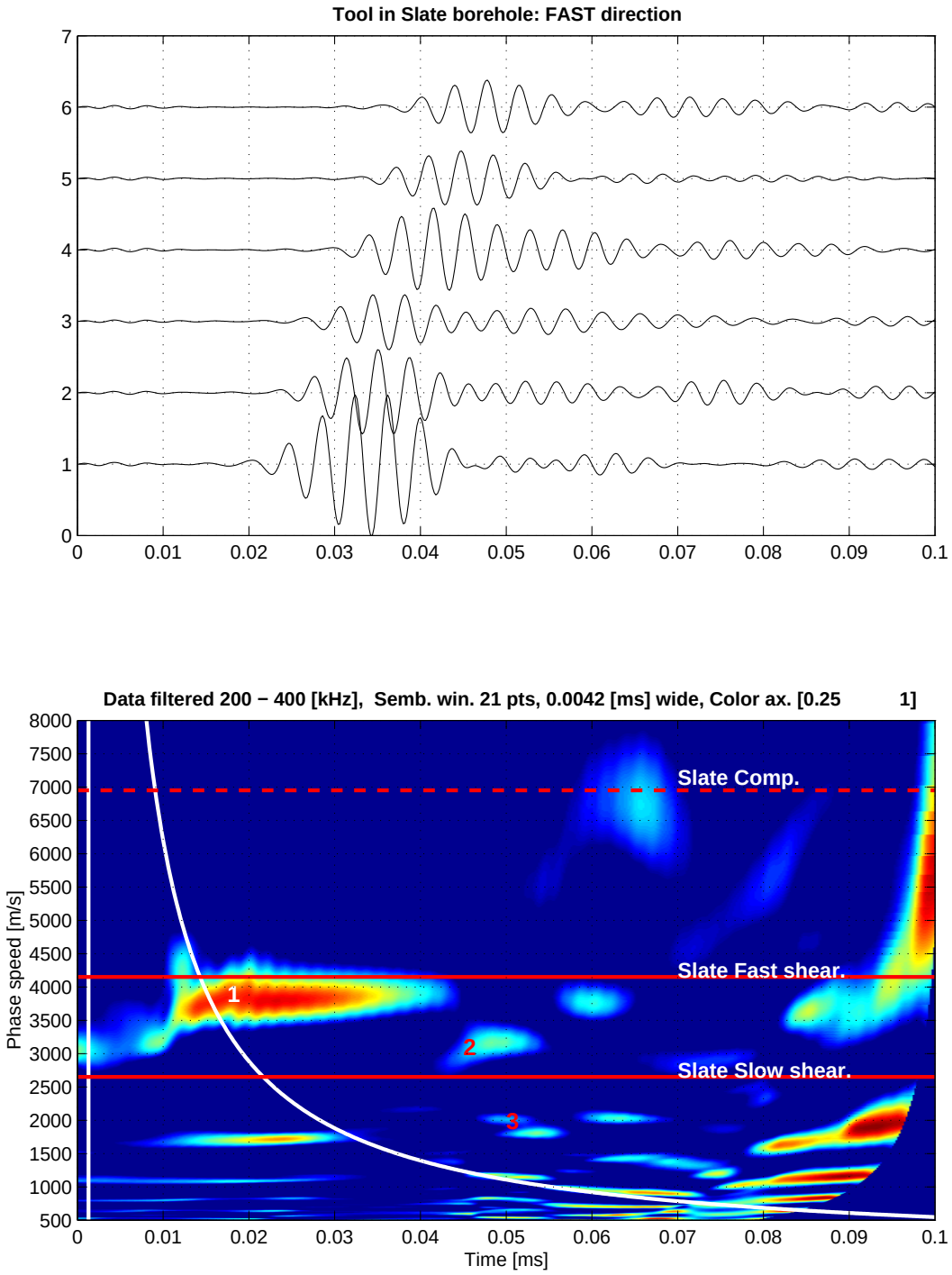

Figure 10: Source and receivers aligned in the fast shear direction in a slate borehole: Measured waveforms and semblance. The locus where phase speed is equal to group speed is identified by the white curve.

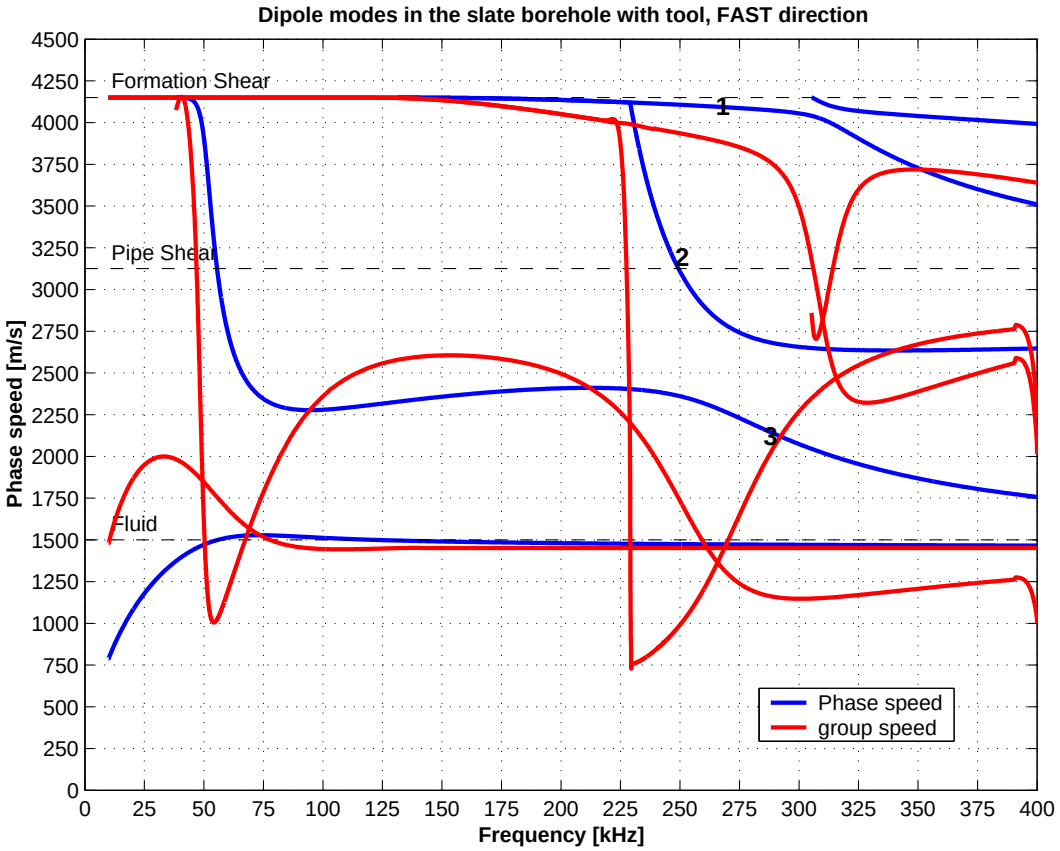

Figure 11: Dipole modes in an isotropic formation with tool, with formation shear speed equal to the fast shear speed of slate and compression speed equal to that of slate.

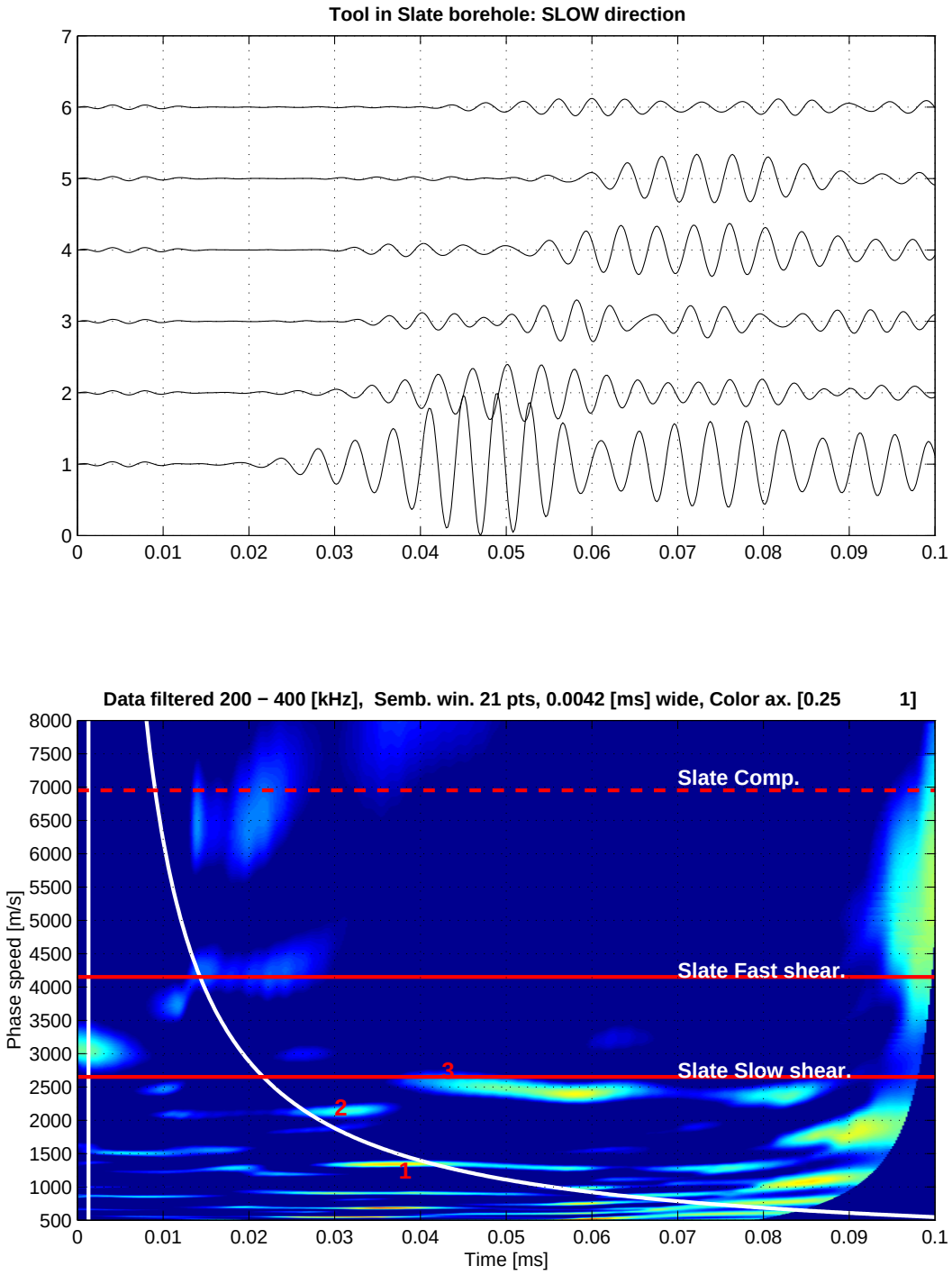

Figure 12: Source and receivers aligned in the slow shear direction in a slate borehole: Measured waveforms and semblance. The locus where phase speed is equal to group speed is identified by the white curve.

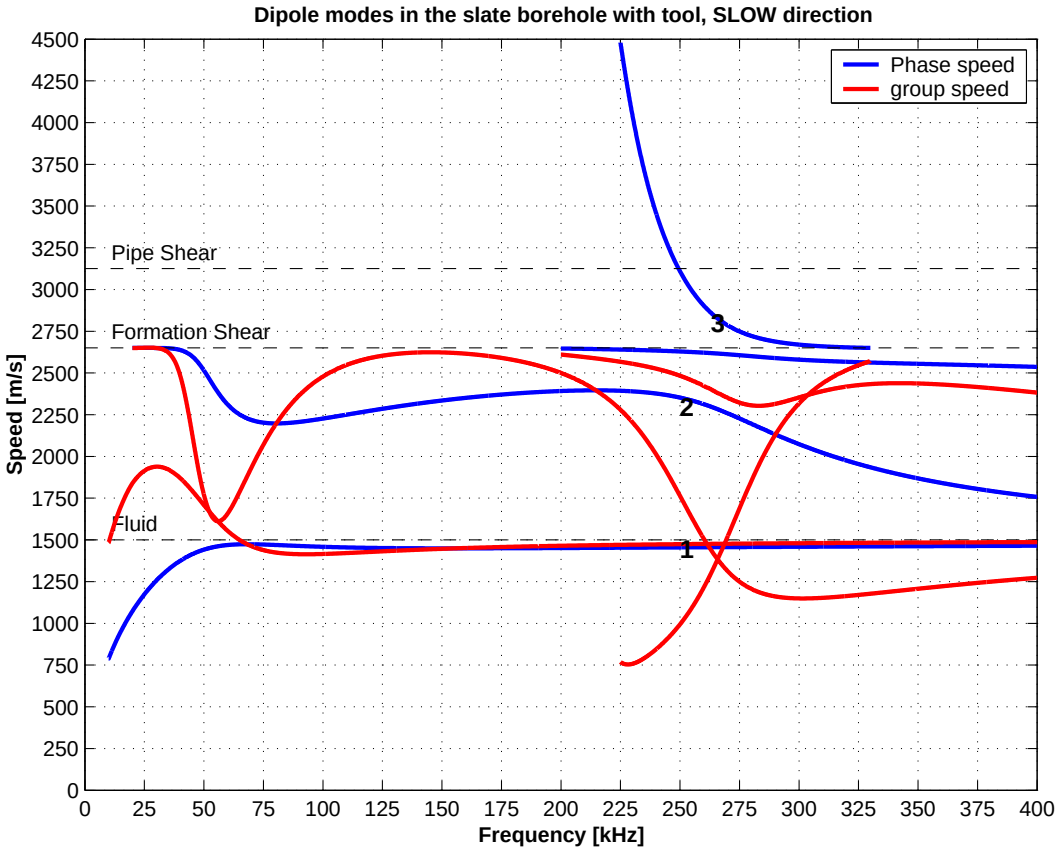

Figure 13: Dipole modes in an isotropic formation with tool, with formation shear speed equal to the slow shear speed of slate and compression speed equal to that of slate.

3.2.2 Slow shear direction

When the source and receivers are aligned in the slow shear direction, the observed waveforms and the corresponding semblance analysis is shown in Figure 12.

The dominant wave packet that propagates across the receiver array, starting at 0.045 ms in the first receiver, corresponds to the semblance peak at 1350 m/s and 0.037 ms (peak 1 in Figure 12). This corresponds to the mode labeled 1 in Figure 13, whose properties are governed by the flexural behavior of the annulus fluid column.

The semblance peaks 2 and 3 correspond to the flexural modes labeled 2 and 3 in Figure 13. Similar to the fast shear direction, two branches together define the flexural behavior of the fluid column inside the tool.

Further, weak semblance peaks corresponding to refracted compression and fast shear are apparent at early times, along the white curve. These direct refracted arrivals were obscured by the strong early arrivals when the source and receiver were oriented in the fast shear direction. The presence of the tool in the borehole has eliminated the obvious arrivals corresponding to the fast shear direction in the slow shear direction measurement. Given that cross modes are not present when measuring with the model tool, it is less likely that they will be present when measuring along principal directions in a real tool (refer Section 3.1.2). This would have to be confirmed with real field data.

Overall, the phase speed/group delay combinations observed in the semblance space compared reasonably to predictions. The discrepancies between the two are likely from the model, i.e., assuming that an anisotropic formation can be modeled as being isotropic when insonified along the principal directions and from potential errors in measuring the slate properties.

4 Conclusions

In an anisotropic fluid-filled borehole with a dipole source and dipole receiver oriented along the principal directions, the flexural modes are the main arrivals. Weak compression and shear refracted arrivals are also discernable when they were not obscured by stronger arrivals. Modes corresponding to fast shear direction are evident in the slow shear direction measurement and not vice versa.

With a model LWD tool in the fluid-filled borehole, and oriented in the fast and slow directions, the main arrivals were the corresponding flexural modes. With the tool in the borehole, the fast shear modes are no longer evident in the slow shear direction. This cross-talk could be function of the source frequency and requires further investigation. The presence of the tool was evident in both measurements (fast and slow direction) in the form of inner fluid column flexural mode arrivals. Additional flexural modes corresponding to the annulus fluid column and the borehole were observed in the slow and fast directions respectively. Thus, these preliminary experiments suggest that with an LWD tool in an anisotropic formation, arrivals sensitive to formation properties can be discerned.

5 Acknowledgments

We would like to thank Prof. Dale Morgan for his valuable suggestions and discussions. This work was supported by the M.I.T. Earth Resources Laboratory Borehole and Acoustics Logging Consortium, and by DOE Grant DE-FG02-00ER15041.

References

R. M. Alford. Shear data in the presence of azimuthal anisotropy. *SEG 56th Annual International Meeting, Expanded Abstracts*, pages 476–479, 1986.

V. Briggs, X. Huang, V. N. R. Rao, and D. R. Burns. Semblance analysis:. *Borehole Acoustics and Logging and Reservoir Delineation Consortia - Annual Report*, 2002.

S. T. Chen. Shear wave logging with dipole source. *Geophysics*, 53:659–667, 1988.

C. H. Cheng and M. N. Toksöz. Elastic wave propagation in a fluid-filled borehole and synthetic acoustic logs. *Geophysics*, 46:1042–1053, 1981.

C. Esmersoy, K. Koster, M.Williams, A. Boyd, and M. Kane. Dipole shear anisotropy logging. *SEG 64th Ann. Internat. Mtg., Expanded Abstracts*, pages 1139–1142, 1994.

A. L. Kurkjian and S. K. Chang. Acoustic multipole sources in fluid-filled boreholes. *Geophysics*, 51:148–163, 1986.

V. N. R. Rao, D. R. Burns, and M. N. Toksöz. Models in LWD applications. *Borehole Acoustics and Logging and Reservoir Delineation Consortia - Annual Report*, 1999.

V. N. R. Rao and J. K. Vandiver. Acoustics of fluid-filled boreholes with pipe: Guided propagation and radiation. *J. Acoust. Soc. Am*, 105:3057–3066, 1999.

B. K. Sinha, A. N. Norris, and S. K. Chang. Borehole flexural modes in anisotropic formation. *Geophysics*, 59:1037–1052, 1994.

L. Tsang and D. Rader. Numerical evaluation of the transient acoustic waveform due to a point source in a fluid-filled borehole. *Geophysics*, 44:1706–1720, 1979.

M. E. Willis and M. N. Toksöz. Automatic p and s velocity determination from full waveform digital acoustic logs. *Geophysics*, 48:1631–1644, 1983.

G. A. Winbow. Seismic sources in open and cased boreholes. *Geophysics*, 56:1040–1050, 1991.

Z. Zhu, C. H. Cheng, and M. N. Toksöz. Propagation of flexural waves in an azimuthally anisotropic borehole model. *SEG 63rd International Meeting Expanded Abstracts*, pages 68–71, 1993.